

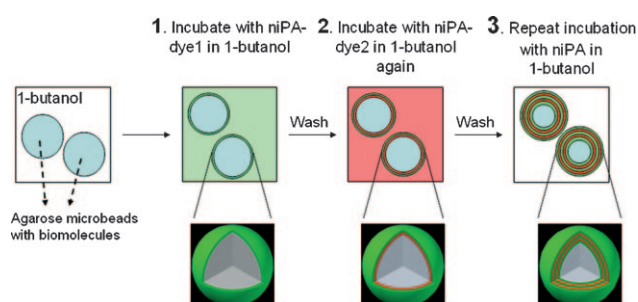
# Inwards Buildup of Concentric Polymer Layers: A Method for Biomolecule Encapsulation and Microcapsule Encoding\*\*

Jianhao Bai, Sebastian Beyer, Wing Cheung Mak, Raj Rajagopalan, and Dieter Trau\*

The phenomenon of polyelectrolytes being able to form complexes with each other have allowed researchers to achieve fabrication of hydrogel particles from these polyelectrolyte complexes,<sup>[1]</sup> gene delivery,<sup>[2]</sup> and fabrication of ultra-thin polymeric multilayers.<sup>[3]</sup> Fabrication of these polyelectrolyte multilayers by the layer-by-layer (LbL) technique is now used regularly for the encapsulation of biomolecules within microcapsules.<sup>[4]</sup> Encapsulation of biomolecules, such as proteins<sup>[5]</sup> and DNA,<sup>[6]</sup> within microcapsules can be used for many biomedical applications, which include but are not limited to biosensors,<sup>[7]</sup> bioreactors,<sup>[8]</sup> and cell targeting<sup>[9]</sup> and release applications.<sup>[10]</sup> Although many microcapsule fabrication techniques have been developed for the encapsulation of biomolecules, to our knowledge, none of these techniques demonstrate the simultaneous capability of encoding.

Herein we present the inwards buildup of concentric colored polymeric layers for the fabrication of striated multicolored spherical shells within agarose microbeads. These shells can simultaneously encapsulate biomolecules within and encode the microbeads. Using a hydrogel as microcapsule core material can provide a favorable environment for biomolecules and maintain the spherical shape of microcapsules.

Encoding of the microcapsules is achieved through color and layer thickness permutation, thereby providing up to two levels of encoding for each microcapsule. These concentric polymer layers form in both agarose and alginate microbeads (Supporting Information, Figure S1) dispersed in 1-butanol. However, for the ease of comparing encoding and encapsulation, in the following, only those results obtained from agarose microbeads will be described. The general steps for the inwards buildup of concentric colored polymer layers into the matrices of agarose microbeads are shown in Scheme 1. Agarose microbeads containing the



**Scheme 1.** The inwards buildup of concentric colored polymer layers into the matrices of agarose microbeads for the encapsulation of biomolecules and encoding. The polymer used is non-ionized poly(allylamine) (niPA).

desired biomolecules to be encapsulated are first dispersed in 1-butanol. An organic solvent was used so as to minimize loss of pre-loaded biomolecules<sup>[11]</sup> during the fabrication process that forms the striated shells. Next, fluorescence-labeled non-ionic (free base) poly(allylamine) (niPA) in 1-butanol is added to the microbead suspension and the first concentric colored layer is formed. The microbeads are then washed with 1-butanol and incubated with another fluorescence-labeled niPA in 1-butanol to form the second concentric colored layer. This incubation and washing process is repeated until the desired number and permutation of concentric colored layers for encoding purpose is obtained (non-fluorescently labeled niPA can also be used for the color encoding, which leads to a non-colored layer). Interestingly, discrete multiple polymer layers can be observed to build up inwards into each agarose microbead matrix by repeated incubation of niPA. As a final step, the striated multicolored polymeric shells are stabilized by cross-linking with disuccinimidyl suberate (DSS) before transferring into 0.01 × PBS (phosphate buffered saline).

Overlaid bright-field and confocal images of agarose microbeads in 1-butanol, with different numbers of concentric

[\*] Prof. R. Rajagopalan, Dr. D. Trau  
Department of Chemical & Biomolecular Engineering  
National University of Singapore  
Engineering Drive 1, 117576 (Singapore)  
Fax: (+65) 6872-3069  
E-mail: bietrau@nus.edu.sg  
Homepage: <http://www.biosingapore.com>

J. Bai, S. Beyer, Dr. D. Trau  
Division of Bioengineering  
National University of Singapore  
Engineering Drive 1, 117574 (Singapore)

S. Beyer  
NUS Graduate School for Integrative Sciences and Engineering  
National University of Singapore  
28 Medical Drive, 117456 (Singapore)

Dr. W. C. Mak  
Department of Chemistry  
Hong Kong University of Science and Technology  
Hong Kong SAR (P.R. China)

[\*\*] This work was supported by Research Grant R-397-000-077-112 from the National University of Singapore (NUS). We thank Colin Sheppard and Lu Fa Ke of the Bioimaging Laboratory, NUS, for assistance and use of the confocal microscope. We are grateful for the comments raised by the anonymous referees that allowed us to improve this work.

Supporting information for this article is available on the WWW under <http://dx.doi.org/10.1002/anie.200906498>.

colored layers and fabricated with fluorescently labeled niPA, are shown in Figure 1. The first colored concentric layer is formed by incubation with niPA-FITC (Figure 1 A), whereas

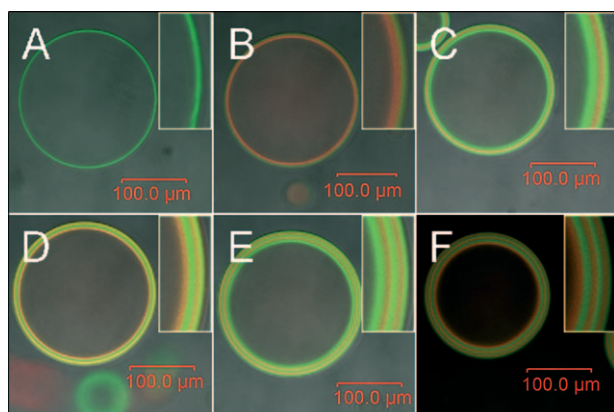


**Figure 1.** Overlay of optical transmission and confocal fluorescence images of agarose microbeads with different number of niPA concentric layers: A) one layer (niPA-FITC), B) two layers (niPA-FITC/niPA-TRITC), C) three layers (niPA-FITC/niPA-TRITC/niPA-FITC), D) four layers ((niPA-FITC/niPA-TRITC)<sub>2</sub>), E) five layers ((niPA-FITC/niPA-TRITC)<sub>2</sub>/niPA-FITC), and F) six layers ((niPA-FITC/niPA-TRITC)<sub>3</sub>). Insets: magnified images of the fluorescence layers. FITC = fluorescein isothiocyanate, TRITC = tetramethylrhodamine isothiocyanate.

the second layer is formed with niPA-TRITC (Figure 1 B). This incubation process is repeated sequentially with niPA-FITC and niPA-TRITC to form agarose microcapsules with 3, 4, 5, and 6 internal concentric colored layers (Figure 1 C,D,E, and F, respectively). These sequential images clearly show that the concentric colored layers always form from the interior surface of previously formed layer(s); that is, the concentric colored layers are built up inwards.

The inwards buildup of colored concentric layers is based on the diffusion of niPA solubilized in an organic solvent (solubility in 1-butanol about 2.5 mg mL<sup>-1</sup>) into the peripheral matrices of agarose microbeads, which is driven by a concentration gradient between the external solution and internal agarose matrix. Upon diffusing, the niPA (solubility in water more than 200 mg mL<sup>-1</sup>) will form complexes with the agarose polymers (Supporting Information, Figure S2) by adsorption.<sup>[12]</sup> It is worth noting that the fundamentals involved in the inwards buildup of concentric polymer layers is in contrast to previous work on active transport of linear polyions into oppositely charged hydrogels,<sup>[13]</sup> and is also different from the outwards buildup of LbL layers.

Comparing our fabricated polymer-hydrogel layers with those formed from linear polyions actively transported into oppositely charged polyelectrolyte hydrogels,<sup>[13,14]</sup> it can be seen that both describe a layered and stable (Supporting Information, Figure S3) polymer-hydrogel complex within the hydrogel, and occupation of the entire hydrogel volume by the polymer (Supporting Information, Figure S4). However, there are fundamental differences that distinguish our current work. The microbeads do not exhibit significant shrinking after two weeks of incubation with excess niPA solution (Supporting Information, Figure S5). Furthermore,

the direction of polymeric layer growth is inwards after passing through previously formed layers, and not by a “relay-race” migration<sup>[13b]</sup> of polymeric layers by which a bound polymer is substituted and forced inwards by a new incoming polymer. Therefore, the direction of layer growth in our experiments strongly suggests that the inwards buildup of concentric polymer layers is a result of niPA diffusing inwards, passing any niPA-agarose complex, and forming a complex with the next free agarose polymer.

We observed an almost constant fluorescence intensity of the layers (Supporting Information, Figure S6), which leads to the conclusion that the concentration of the formed agarose niPA complex is constant within layers at any point of the microbead and suggests a constant capacity of the agarose to form the complex with niPA. The thickness of each concentric layer can be tuned by varying the amount of niPA present during incubation (Figure 2 A) or by changing the incubation time (Figure 2 B) (only microcapsules with diameters of about

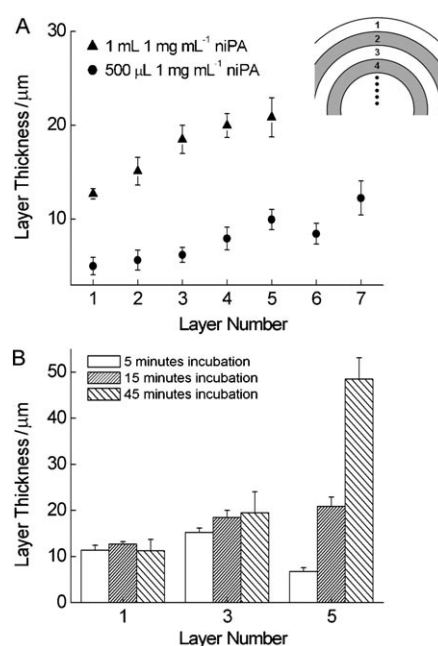


**Figure 2.** Layer thickness of concentric layers as a function of layer number, amount of polymer, and incubation time. A) Doubling the niPA volume causes an increase in concentric layer thickness for same incubation time (15 min). Inset: visual definition of layer number. B) Layer thickness for the first, third, and fifth layer as a function of incubation time at constant volume and niPA concentration.

175 μm were analyzed). It can be observed that the layer thickness increases when 1) the layer number increases, 2) the agarose microbeads are exposed to a larger quantity of niPA, and 3) the incubation time is increased. Only the thickness of the first layer does not increase when the incubation time is changed, which indicates that equilibrium is attained. Because subsequent layers can be formed, and 90 % of the polymer was consumed from the supernatant solution for the first layer (Supporting Information, Figure S7), it can be concluded that the process was limited by the amount of

available niPA polymer. This explains why an increase in polymer volume causes an increase in the layer thickness. For the formation of all the layers, the concentration of the polymer will decrease with progressing incubation time and therefore the inwards diffusion rate of polymer will decrease. This decrease in diffusion rate will be less for increasing volumes of polymer solution, which explains the formation of thicker layers for larger volumes of polymer solution even for cases in which equilibrium is not reached. However, the mechanism is further complicated, because with build-up of more layers, the diffusion barrier increases (which should cause a reduction in layer thickness), and the inner free available volume decreases (which should cause an increase in layer thickness). Our observations demonstrate that the polymer volume effect prevails and layer thickness increases with layer number (Figure 2 A). To demonstrate the double encoding capability, striated shells of different color and thickness permutation were fabricated (Supporting Information, Figure S8).

The permeability of the multilayer capsules was studied using dextran-TRITC (65 000–76 000 Da) as it cannot be cross-linked by DSS and is a non-charged polymer. Figure 3 shows the distribution of dextran-TRITC within agarose microbeads of one (Figure 3 A,D), three (Figure 3 B,E), and five (Figure 3 C,F) cross-linked concentric colored layers.

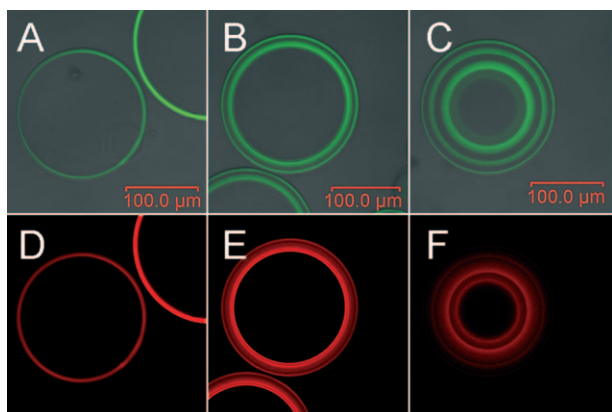


**Figure 3.** A–C) Overlay of optical transmission and confocal FITC fluorescence images of agarose microcapsules encapsulating dextran-TRITC with: A) one layer of niPA-FITC, B) three concentric layers of niPA-FITC/niPA/niPA-FITC, and C) five concentric layers of (niPA-FITC/niPA)<sub>2</sub>/niPA-FITC. D–F) Confocal TRITC fluorescence images of the encapsulated dextran-TRITC (65 000–76 000 Da) in agarose microbeads of D) one layer, E) three concentric layers, and F) five concentric layers.

Dextran-TRITC is entrapped within regions where the cross-linked niPA resides and is not homogeneously distributed in the center. This non-homogeneous distribution of encapsulated dextran was also reported in hollow LbL microcapsules.<sup>[15]</sup> Therefore, as dextran-TRITC cannot be cross-linked by DSS, is non-charged, and is distributed within the core of the agarose microcapsules (Supporting Information, Figure S9), the dextran is likely to have been physically “entangled” and entrapped within the cross-linked niPA shells. This entrapment occurred when the microcapsules

were transferred from 1-butanol to an aqueous phase; a concentration gradient was established between the interior and exterior aqueous environment of the microcapsules, thus creating a driving force for the dextran to diffuse out.

To demonstrate that encapsulated biomolecules can retain their biofunctionality after going through the fabrication process, glucose oxidase (GOx) and horseradish peroxidase (HRP) were encapsulated within microcapsules of three cross-linked concentric layers, namely colorless/green/colorless and colorless/red/colorless, respectively. Bovine serum albumin (BSA) was also encapsulated as a control (red/colorless/green). The three different types of microcapsules were subsequently mixed together to form two different sets of microcapsules: set 1 (HRP and BSA microcapsules; Figure 4 A,D) and set 2 (HRP and GOx microcapsules; Fig-

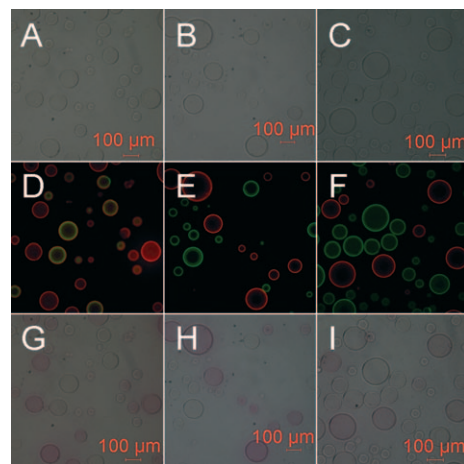


**Figure 4.** Demonstration of enzymatic viability in microcapsules encapsulating HRP (labeled red only) and encapsulating GOx (labeled green only). BSA microcapsules were used as a control (labeled green and red). Optical transmission images of A) HRP and BSA microcapsules, B,C) HRP and GOx microcapsules, and corresponding overlapping FITC and TRITC fluorescence images of D) HRP and BSA microcapsules and E,F) HRP and GOx microcapsules before addition of substrates. G,H) Addition of H<sub>2</sub>O<sub>2</sub> and Ampliflu Red (AR) to the HRP and BSA microcapsules (G) and HRP and GOx microcapsules (H). After 10 seconds, only the HRP microcapsules were observed to turn purple. I) Addition of glucose and AR to the HRP and GOx microcapsules. After two minutes, only the HRP microcapsules turned purple.

ure 4 B,C,E,F). Biofunctionality of encapsulated GOx and HRP was demonstrated by enzymatic activity measurements after addition of glucose/Ampliflu Red (AR) for GOx and hydrogen peroxide (H<sub>2</sub>O<sub>2</sub>)/AR for HRP. In the presence of oxygen, GOx converts glucose into gluconolactone and H<sub>2</sub>O<sub>2</sub>; in the presence of H<sub>2</sub>O<sub>2</sub>, HRP converts AR into a purple-colored product. Figure 4 G,H shows the color that is observed 10 seconds after addition of H<sub>2</sub>O<sub>2</sub>/AR to HRP/BSA and HRP/GOx microcapsules, respectively, and glucose/AR addition to HRP/GOx microcapsules is shown in Figure 4 I.

From the color permutations, it can be decoded that the purple product is observed only for the HRP microcapsules



(Figure 4G,H), thus indicating that HRP can retain its biofunctionality after going through the fabrication process. Figure 4I shows the color formation two minutes after addition of glucose/AR. After similar decoding, the purple product is only observed at the HRP microcapsules; GOx had therefore also retained its biofunctionality. A longer time was necessary for the enzymatic assay of the (glucose/AR/HRP/GOx) set to form the colored product, as time was required for the  $\text{H}_2\text{O}_2$  produced by the GOx microcapsules to diffuse to the HRP microcapsules.

In conclusion, we have demonstrated the encapsulation of biomolecules within microcapsules encoded with a color/thickness scheme. The encapsulation and encoding process was performed through an inwards buildup of concentric colored layers to create a striated multicolored polymeric shell; the colors and thickness of these layers can be permuted to give two levels of encoding possibilities. GOx and HRP were used to demonstrate that biomolecules can be encapsulated within these microcapsules, and they retained their biofunctionality. We believe that this novel approach can greatly contribute to the field of colloidal science and engineering and microencapsulation, for example with microcapsule identification in solution or in bioarrays for multiplexed biodetections or bioreactions. Furthermore, we envision incorporating different chemical or biological functionalities within each layer to carry out and possibly visualize different types of reactions within a hydrogel environment and in a layered manner.

## Experimental Section

Dextran-TRITC Mw 65 000–76 000 Da, 1-butanol anhydrous 99.8%, disuccinimidyl suberate (DSS), fluorescein isothiocyanate (FITC), glucose oxidase (GOx), horseradish peroxidase (HRP), bovine serum albumin (BSA), D-(+)-glucose, and mineral oil were purchased from Sigma; Span 80, Ampliflu Red, and tetramethylrhodamine isothiocyanate (TRITC) were purchased from Fluka; 1-undecanol, calcium iodide ( $\text{CaI}_2$ ), poly(allylamine) (PA;  $M_w$  65 000 Da), and ADOGEN 464 were purchased from Aldrich; low-melting agarose was purchased from Promega; ethanol was purchased from Fisher Scientific; PBS was purchased from 1st Base; and chloroform and hydrogen peroxide ( $\text{H}_2\text{O}_2$ ) were purchased from BDH chemicals. Water was doubly distilled as required using a Fiestreem Cyclone (UK) apparatus.

Non-ionized poly(allylamine) (niPA) in 1-butanol was prepared by drying the purchased PA solution and fully saturating 1-butanol with the dried PA. The saturated 1-butanol (1 mL) was dried with and weighed, and the solution was then diluted with 1-butanol to prepare a  $1 \text{ mg mL}^{-1}$  niPA solution. Fluorescence-labeled niPA was prepared by dissolving and reacting FITC or TRITC with niPA in 1-butanol at a fluorescence monomer/PA monomer ratio of 1:100.

Agarose microbeads were prepared by adding a 2% w/v low-melting agarose in doubly distilled  $\text{H}_2\text{O}$  (with the desired biomolecules if required) pre-warmed at  $45^\circ\text{C}$  to mineral oil at  $45^\circ\text{C}$  containing 0.1% Span 80, and stirred to form water-in-oil emulsion droplets. The droplets were then cooled in an ice water bath with stirring to solidify the molten droplets into agarose microbeads, which were further stabilized by cooling to  $-20^\circ\text{C}$ . Alginate microbeads were prepared by adding 2% w/v alginate in doubly distilled  $\text{H}_2\text{O}$  to mineral oil containing 0.1% Span 80 and stirred to form water-in-oil emulsion droplets. An equal volume of 1-undecanol containing 0.05 M  $\text{CaI}_2$  was then added to the emulsion and incubated for 15 min to allow the alginate to gelate. The volume ratio between the water and oil phase was 1:25.

To transfer the agarose or alginate microbeads from oil to 1-butanol, ethanol containing 0.5% ADOGEN 464 was added to the agarose or alginate microbead-in-oil suspension and mixed vigorously, followed by centrifugation. The mineral oil and ethanol supernatant was then discarded and the pellet containing the agarose or alginate microbeads was washed with 1-butanol containing 0.5% ADOGEN 464. The resulting agarose or alginate microbeads were then incubated with the desired amount niPA or niPA-TRITC or niPA-FITC in 1-butanol containing 0.5% ADOGEN 464 for the desired time under gentle vortexing, followed by removal of excess niPA and washing with 1-butanol. Typically, 200  $\mu\text{L}$  beads were incubated with 1 mL of the niPA solution, which forms the first concentric layer of niPA. The incubation with niPA solution containing 0.5% ADOGEN 464 was then repeated to form the second and following layers until the desired number of concentric niPA layers was reached. (Incubation of niPA without ADOGEN 464 will result in the same concentric layer formation. ADOGEN 464, a cationic surfactant, was included in the fabrication process to ensure that the agarose microbeads do not complex or dehydrate when dispersed in 1-butanol.) To stabilize the concentric layers, the microbeads were then incubated with DSS (40  $\text{mg mL}^{-1}$  in chloroform) for 2 h. Cross-linking is necessary as most of the layer forming niPA would otherwise dissolve and disperse once the microbeads are transferred into an aqueous dispersant. To transfer the agarose microcapsules from 1-butanol to PBS, the agarose microcapsules were first washed twice with ethanol and then with PBS/ethanol solutions of increasing PBS content (0.01  $\times$ ; 10%, 50%, and 90%) before transferring to pure 0.01  $\times$  PBS.

Enzymatic analysis of GOx and HRP was performed by using 5  $\text{mg mL}^{-1}$  glucose in  $1 \times$  PBS, 0.02%  $\text{H}_2\text{O}_2$  in  $1 \times$  PBS, and 5  $\text{mg mL}^{-1}$  Ampliflu Red in DMSO.

To determine the concentration of niPA left in the supernatant solution, niPA-FITC (500  $\mu\text{L}$ ,  $1 \text{ mg mL}^{-1}$ ) was used for each layer. The agarose microbeads were centrifuged after incubation and the supernatant was checked for fluorescence using a microplate reader (FLUOstar OPTIMA, BMG LABTECH, Germany). The concentration of niPA-FITC left in the supernatant for each layer was measured by comparing against the stock niPA-FITC solution used.

Phase-contrast and fluorescence images were recorded using a CCD color digital camera (Retiga 4000R, QImaging, Canada) connected to a system microscope (Olympus BX41, Japan). Images were captured with QCapture Pro software (Version 5.1.1.14, QImaging, Canada). Confocal fluorescence microscopic images were captured using a laser scanning confocal microscope (FluoView FV300, Olympus, Japan) and analyzed by ImageJ software (Scion Corp., USA).

Received: November 18, 2009

Revised: April 19, 2010

Published online: June 16, 2010

**Keywords:** encapsulation · encoding · hydrogels · microcapsules · polyelectrolytes

- [1] a) V. Štefuca, P. Gemeiner, L. Kurillaová, H. Dautzenberg, M. Polakovič, V. Bálaš, *Appl. Biochem. Biotechnol.* **1991**, *30*, 313–324; b) C. Schatz, J. Lucas, C. Viton, A. Domard, C. Pichot, T. Delair, *Langmuir* **2004**, *20*, 7766–7778.
- [2] a) S. C. De Smedt, J. Demeester, W. E. Hennink, *Pharm. Res.* **2000**, *17*, 113–126; b) H. Dautzenberg, A. Zintchenko, *Langmuir* **2001**, *17*, 3096–3102.
- [3] a) G. Decher, J. D. Hong, J. Schmitt, *Thin Solid Films* **1992**, *210/211*, 831–835; b) G. Decher, *Science* **1997**, *277*, 1232–1237.
- [4] a) F. Caruso, D. Trau, H. Möhwald, R. Renneberg, *Langmuir* **2000**, *16*, 1485–1488; b) C. Gao, E. Donath, H. Möhwald, J. Shen, *Angew. Chem.* **2002**, *114*, 3943–3947; *Angew. Chem. Int.*

- Ed.* **2002**, *41*, 3789–3793; c) R. Georgieva, S. Moya, M. Hin, R. Mitlöhner, E. Donath, H. Kieseewetter, H. Möhwald, H. Bäuml, *Biomacromolecules* **2002**, *3*, 517–524; d) C. S. Peyratout, L. Dähne, *Angew. Chem.* **2004**, *116*, 3850–3872; *Angew. Chem. Int. Ed.* **2004**, *43*, 3762–3783; e) K. Köhler, G. B. Sukhorukov, *Adv. Funct. Mater.* **2007**, *17*, 2053–2061; f) J. Bai, S. Beyer, W. C. Mak, D. Trau, *Soft Matter* **2009**, *5*, 4152–4160.
- [5] a) A. Yu, Y. Wang, E. Barlow, F. Caruso, *Adv. Mater.* **2005**, *17*, 1737–1741; b) B. Samanta, X. Yang, Y. Ofir, M. Park, D. Patra, S. S. Agasti, O. R. Miranda, Z. Mo, V. M. Rotello, *Angew. Chem.* **2009**, *121*, 5445–5448; *Angew. Chem. Int. Ed.* **2009**, *48*, 5341–5344; c) B. Städler, R. Chandrawati, A. D. Price, S. Chong, K. Breheny, A. Postma, L. A. Connal, A. N. Zelikin, F. Caruso, *Angew. Chem.* **2009**, *121*, 4423–4426; *Angew. Chem. Int. Ed.* **2009**, *48*, 4359–4362.
- [6] a) O. Kreft, R. Georgieva, H. Bäuml, M. Steup, B. Müller-Röber, G. B. Sukhorukov, H. Möhwald, *Macromol. Rapid Commun.* **2006**, *27*, 435–440; b) A. N. Zelikin, Q. Li, F. Caruso, *Angew. Chem.* **2006**, *118*, 7907–7909; *Angew. Chem. Int. Ed.* **2006**, *45*, 7743–7745.
- [7] a) J. Q. Brown, R. Srivastava, M. J. McShane, *Biosens. Bioelectron.* **2005**, *21*, 212–216; b) O. Kreft, A. M. Javier, G. B. Sukhorukov, W. J. Parak, *J. Mater. Chem.* **2007**, *17*, 4471–4476.
- [8] a) O. Kreft, A. G. Skirtach, G. B. Sukhorukov, H. Möhwald, *Adv. Mater.* **2007**, *19*, 3142–3145; b) W. C. Mak, K. Y. Cheung, D. Trau, *Adv. Funct. Mater.* **2008**, *18*, 2930–2937.
- [9] a) M. Fischlechner, O. Zschörnig, J. Hoffman, E. Donath, *Angew. Chem.* **2005**, *117*, 2952–2955; *Angew. Chem. Int. Ed.* **2005**, *44*, 2892–2895; b) C. Cortez, E. Tomaskovic-Crook, A. P. R. Johnston, B. Radt, S. H. Cody, A. M. Scott, E. C. Nice, J. K. Heath, F. Caruso, *Adv. Mater.* **2006**, *18*, 1998–2003.
- [10] A. G. Skirtach, A. M. Javier, O. Kreft, K. Köhler, A. P. Alberola, H. Möhwald, W. J. Parak, G. B. Sukhorukov, *Angew. Chem.* **2006**, *118*, 4728–4733; *Angew. Chem. Int. Ed.* **2006**, *45*, 4612–4617.
- [11] a) S. Beyer, W. C. Mak, D. Trau, *Langmuir* **2007**, *23*, 8827–8832; b) W. C. Mak, J. Bai, X. Y. Chang, D. Trau, *Langmuir* **2009**, *25*, 769–775.
- [12] G. J. Fleer, M. A. Cohen Stuart, J. M. H. M. Scheutjens, T. Cosgrove, B. Vincent in *Polymers at Interfaces*, Chapman & Hall, London, **1993**, chap. 2, pp. 27–42.
- [13] a) V. B. Rogacheva, V. A. Prevish, A. B. Zezin, V. A. Kabanov, *Polym. Sci. U.S.S.R.* **1988**, *30*, 2262–2270; b) V. A. Kabanov, A. B. Zezin, V. B. Rogacheva, V. A. Prevish, *Makromol. Chem.* **1989**, *190*, 2211–2216; c) A. B. Zezin, V. B. Rogacheva, V. A. Kabanov, *J. Intell. Mater. Syst. Struct.* **1994**, *5*, 144–146.
- [14] a) V. A. Kabanov, V. B. Skobeleva, V. B. Rogacheva, A. B. Zezin, *J. Phys. Chem. B* **2004**, *108*, 1485–1490; b) K. T. Oh, T. K. Bronich, V. A. Kabanov, A. V. Kabanov, *Biomacromolecules* **2007**, *8*, 490–497.
- [15] a) A. A. Antipov, G. B. Sukhorukov, S. Leporatti, T. L. Radtchenko, E. Donath, H. Möhwald, *Colloid Surf. Physicochem. Eng. Aspects* **2002**, *198*, 535–541; b) D. V. Volodkin, A. I. Petrov, M. Prevot, G. B. Sukhorukov, *Langmuir* **2004**, *20*, 3398–3406.